1   This manuscript is textually identical with the published paper:

7

8   Niche differentiation among invasive Ponto-Caspian *Chelicorophium* species (Crustacea, Amphipoda,

9   Corophiidae) by food particle size

10

11   Péter Borza[1,2*], Thomas Huber[3], Patrick Leitner[3], Nadine Remund[4], Wolfram Graf[3]

12

13   [1]GINOP Sustainable Ecosystems Group, MTA Centre for Ecological Research, Klebelsberg Kuno utca

14   3, H-8237 Tihany, Hungary

15   [2]Danube Research Institute, MTA Centre for Ecological Research, Karolina út 29-31, H-1113

16   Budapest, Hungary

17   [3]Department of Water, Atmosphere & Environment, Institute for Hydrobiology & Water Management,

18   BOKU - University of Natural Resources and Applied Life Sciences, Gregor Mendel Strasse 33, A-

19   1180 Vienna, Austria

20   [4]Info fauna – CSCF, Passage Maximilien-de-Meuron 6, CH-2000 Neuchâtel, Switzerland

21   [*] E-mail: borza.peter@okologia.mta.hu, tel: +361-279-3100/306

22

23   Acknowledgements

24

35

36   Abstract

37

38   After *Chelicorophium curvispinum*, two other Ponto-Caspian tube-dwelling, filter feeding amphipod

39   species (*C. robustum* and *C. sowinskyi*) have colonized several catchments in Central and Western

40   Europe in recent decades. To reveal the mechanism of niche differentiation among them, we measured

41   the mesh sizes of their filtering apparatus and analyzed multi-habitat sampling data from the River

42   Danube using RDA-based variance partitioning between environmental and spatial explanatory

43   variables. Morphometric data showed clear differentiation among the species by filter mesh size (*C.*

44   *curvispinum* > *C. robustum* > *C. sowinskyi*). Field data also indicated the relevance of suspended

45   matter; however, the mere quantity of suspended solids included in the analysis could not explain the

46   abundance patterns effectively. Current velocity, substrate types, and total nitrogen content also had a

47   non-negligible effect; however, their role in the niche differentiation of the species is not evident. In

48   summary, differences in their filter mesh sizes indicate a niche differentiation by food particle size

49   among the invasive *Chelicorophium* species, allowing their stable coexistence given sufficient size

50   variability in their food source. Consequently, the two recent invaders increase the effectiveness of

51   resource utilization, resulting in a more intensive benthic-pelagic coupling in the colonized

52   ecosystems.

53

54   Keywords

55

56   benthic-pelagic coupling, filter feeding, invasion impact, River Danube, suspended matter

57

Introduction

59

Suspension feeding organisms play a key role in aquatic ecosystems by linking the pelagic and benthic

compartments of the food web (Atkinson et al. 2013; Zhang et al. 2016; Griffiths et al. 2017).

Accordingly, the establishment of a filter feeding invader can induce profound changes in the

functioning of both running and still waters (Sousa et al. 2014), well exemplified by the invasion

impact of the Ponto-Caspian dreissenid mussels, implying reduced plankton biomass, increased water

clarity favoring benthic algae and macrophytes, cyanobacterial blooms, increased benthic invertebrate

biomass, and consequent changes in fish assemblages (Higgins and Vander Zanden 2010).

The tube-dwelling euryhaline amphipods of the Ponto-Caspian *Chelicorophium* genus are also

suspension feeders, receiving attention mainly on account of their successful range expansion in

several Central and Western European catchments since the early 20th century. *Chelicorophium*

curvispinum (G.O. Sars, 1895), the first species of the genus to arrive in Western Europe (Bij de Vaate

et al. 2002) had a dramatic impact on the colonized waters, especially in the eutrophic River Rhine.

Here, the species reached extreme high densities in the 1980-90s (Van den Brink et al. 1993), and

formed a thick layer of muddy tubes on hard substrates which suffocated adult *Dreissena* mussels and

prevented the settlement of their larvae, resulting in the decline of the population (Van der Velde et al.

1994). At the same time, the species became an important food source for fish (Kelleher et al. 1998).

Although its abundance had decreased in the Rhine by the 2000s, presumably due to increased

predation pressure after the invasion of *Dikerogammarus villosus* (Sowinsky, 1894) (Van Riel et al.

2006), the species continues to be a key member of benthic macroinvertebrate assemblages in most

invaded waters (Noordhuis et al. 2009; Hellmann et al. 2015).

Recently, two additional representatives of the genus extended their ranges in Central and Western

Europe using the Danube-Rhine system. *Chelicorophium robustum* (G.O. Sars, 1895) – formerly

present in the Danube only downstream of the Serbian river section – was recorded in the River Main

in 2000 (Bernerth et al. 2005). It colonized the Upper and Middle Danube later by downstream drift

(Borza et al. 2015), and recently it was found in the Rhine (Bernauer and Jansen 2006; Altermatt et al.

85   2014) as well as in several connected French waterways (Labat et al. 2011). The third species,

86   *Chelicorophium sowinskyi* (Martynov, 1924) was found in the Middle Danube already in the 1910s

87   (Borza 2011), and recent records confirmed its presence in Austria, Germany, France, and

88   Switzerland, as well (Bernerth and Dorow 2010; Borza et al. 2010; Forcellini 2012; Altermatt et al.

89   2014).

90   Despite their key functional role in aquatic ecosystems, the ecology of the invasive *Chelicorophium*

91   species has received little scientific attention so far. Consequently, the mechanism of niche

92   differentiation among the three species – informative of how the two recent invaders modify the

93   impact of *C. curvispinum* – has not been revealed. Benthic filter feeding species usually compete for

94   food or space (Svensson and Marshall 2015). In the former case, niche differentiation is achieved

95   through partitioning of food sources by particle size (e.g. Lesser et al. 1992; Kang et al. 2009), while

96   in the latter case the species show spatial separation along certain environmental factors, such as

97   substrate properties, current velocity, or water depth (e.g. Brönmark and Malmqvist 1982; Jones and

98   Ricciardi 2005). The two factors cannot be separated in all instances; e.g. hydropsychid caddisflies

99   with larger filter mesh sizes tend to occur in microhabitats with stronger currents (Wallace et al. 1977).

100   In the present study we aimed to reveal the mechanism of niche differentiation among the invasive

101   *Chelicorophium* species by focusing on the two most likely factors. First, we examined whether

102   differences can be observed in the mesh sizes of the filtering apparatus of the three species, suggesting

103   niche differentiation by food particle size. Second, we tested whether certain environmental variables

104   indicate spatial niche differentiation.

105

106   Material and methods

107

108   Morphometric data

109

110   We measured the filter mesh size of the invasive *Chelicorophium* species on microscopic dissections

111   from specimens collected in the Lower Danube, where all three species occur natively (see 'Field data'

112   for details on the sampling). Since abundant materials of all three species – allowing the representation

113   of their full body size spectrum in both genders – were not available from the same site, we included

114   specimens from a site where the three species were present in similar density (river km 104, Sf.

115   Gheorghe arm of the delta), and supplemented the material from sites where the species were abundant

116   (river km 375 for *C. curvispinum* and *C. robustum*, and river km 532 for *C. sowinskyi*; Table 1).

117   The filter of corophiids is formed by two rows of plumose setae on the anterior margin of the merus of

118   the second gnathopod, where the mesh size is determined by the distance between bristles (Riisgård

119   and Larsen 2010: 275, fig. 25-26). To get a clear view on the medially oriented bristles of the distal

120   (apical) row of setae, we carefully removed the medial (subapical) row of setae using a sharp pin

121   under stereomicroscope. We then mounted the detached limbs on a slide and took digital photographs

122   under light microscope with 100-fold magnification. Since the length of bristles appeared to increase

123   toward the end of the setae and the distances between them increased accordingly, we took pictures of

124   the relatively short and densely arranged basal bristles, the distances of which were assumed to

125   provide a good approximation the filtered particle sizes (the long distal bristles can lean in the current,

126   so the actual distances between them might be smaller). To diminish measurement error, we measured

127   the distance between five bristles, which might imply a slight underestimation of the within-individual

128   variation of filter mesh sizes (presented here as the distance between the centers of two neighboring

129   bristles in μm). We made ten independent (i.e. non-overlapping) measurements on each specimen

130   using the tpsdig 2.22 digital picture analysis software (Rohlf 2015).

131

132   Field data

133

134   The field samples analyzed in the present study were collected during the Joint Danube Survey 3 (13

135   August–26 September 2013) at 55 sites of the river between Ulm (river km 2,581) and the Delta (river

136   km 18, Kiliya branch; Fig. 1) by the ’multi-habitat’ approach based on, but not strictly following the

137   AQEM protocol (Hering et al. 2004). At each site, 4-7 samples (altogether 251) consisting of five

138   pooled units covering 25 x 25 cm bottom area were collected in the littoral zone by hand net (aperture:

139   25 x 25 cm, mesh size: 500 μm), representing all available habitat types (Table 2). All samples were

140   preserved in 4% formaldehyde solution in the field, and stored in 70% ethanol after sorting. Sorting

141   was facilitated by fractioning the material on a set of sieves (mesh sizes: 0.5, 2, 5, 10, and 20 mm). In

142   some cases, two to 64-fold subsampling of the smallest one or two fractions was necessary due to the

143   extremely high number of juvenile animals in the samples. *Chelicorophium* specimens (altogether

144   11,451 individuals) could be identified to species level above ~2 mm body length (9,282 ind.);

145   unidentifiable juveniles were omitted. Depth (range: 0.1-1.2 m) and current velocity (0-0.37 m/s;

146   measured at approx. 5 cm from the bottom using Marsh-McBirney Flo-Mate™ Portable Velocity Flow

147   Meter Model 2000) were recorded for each subsample and averaged separately for each site.

148   Conductivity (9.29-566.00 μS/cm), pH (7.89-8.43), dissolved O_2 (5.89-10.42 mg/l), dissolved organic

149   carbon (1.59-7.63 mg/l), total nitrogen (0.52-3.37 mg/l), total phosphorus (0.02-0.11 mg/l), and

150   chlorophyll-a concentration (0.10-18.77 μg/l) were measured at two points per site near the river

151   banks, whereas the concentration suspended matter ('total suspended solids', TSS hereafter; 2.5-50.0

152   mg/l) was recorded at one point per site during the survey.

153

154   Statistical analysis

155

156   We modelled filter mesh sizes in two steps. First, for descriptive purposes, we fitted linear mixed-

157   effects models on each species separately, including standard body length (measured between the tip

158   of the rostrum and the tip of the telson), gender, and sampling site as fixed effects, and individuals as a

159   random effect using the 'nlme' package (Pinheiro et al. 2016) in R 3.2.5 (R Core Team 2016).

160   Following the recommendations of Zuur et al. (2009), we assessed the fit of the models including all

161   explanatory variables and their interactions using diagnostic figures. We then fitted variance functions,

162   if considerable heteroscedasticity was detected (the choice of the function was based on *AIC* and *BIC*

163   scores; the simpler model was preferred in cases of contradiction between the two scores), and after

164   that we omitted non-significant fixed effects step-by-step based on the *t*-statistic (juveniles were

165   included only if 'gender' was omitted). We characterized the optimal models by the parameters as well

166   as the marginal R^2 (fixed effects; $R^2_{GLMM(m)}$) and conditional R^2 (fixed and random effects; $R^2_{GLMM(c)}$)

167   as defined by Nakagawa and Schielzeth (2013), calculated by the 'sem.model.fits' function in the

168 'piecewiseSEM' package (Lefcheck 2016). We interpret among-individual variance (=random effects)

169 as $R^2_{GLMM(c)} - R^2_{GLMM(m)}$, and within-individual (=residual) variance as $1 - R^2_{GLMM(c)}$.

170 Second, to test for interspecific differences, we fitted a linear mixed-effects model on the three

171 species, following the procedure as described for the single-species models. We did not include

172 variables which had proved non-significant in the single-species models..

173 We tested for spatial niche differentiation by variance partitioning between environmental and spatial

174 explanatory variables based on redundancy analysis (RDA), using the 'varpart' function in the 'vegan'

175 package (Oksanen et al. 2017). We used ln(x+1) and Hellinger-transformed (Legendre and Gallagher

176 2001) count data (individuals per sample) in the analysis, but we show ind./m^2 values in the results and

177 in figures for the sake of comparability. We modelled the spatial structure of the study using the

178 asymmetric eigenvector map (AEM) method (Blanchet et al. 2008a; Blanchet et al. 2011) allowing the

179 consideration of directional spatial processes, induced by the currents in our case. Since the locations

180 of the samples within sites were not recorded, we considered only sites, using river km distances (d_{ij})

181 weighted as $1/d_{ij}$ (conforming to Borza et al. 2017a), and replicated the values of the generated

182 spatial variables (AEM eigenfunctions) for all samples within each site. We excluded two sites (8

183 samples) in the two minor arms of the Danube delta (Sulina and Sf. Gheorghe) allowing the one-

184 dimensional representation of the study design including 152 samples from 46 sites (64 samples did

185 not contain *Chelicorophium* species, and 27 additional samples were omitted due to missing values).

186 We used the eigenfunctions both with positive and negative Moran's *I* values (modelling positive and

187 negative spatial autocorrelation, respectively) in the analysis, which was possible due to the fact that

188 we only had 45 (number of sites minus one) AEM eigenfunctions for 152 samples. We performed

189 forward selection (Blanchet et al. 2008b) on the environmental variables with two different adding

190 limits ($P = 0.05$ and 0.01; using the 'ordiR2step' function in the 'vegan' package) to provide more

191 insight into their importance, but we used only the wider set of variables ($P = 0.05$) in variance

192 partitioning. For this, we selected spatial variables with $P = 0.05$ adding limit, as well, and tested

193 variance partitions of interest by ANOVA with 9999 permutations. We present the effect of the

194 environmental variables based on their biplot scores in the model including both environmental and

195 spatial variables. We mapped the environmentally explainable fraction of variance (including the

196 overlap) as well as the only spatially explainable part (without the overlap) by plotting the fitted site

197 scores (= linear constraints; '*LC*' scores) of the first canonical axis in the corresponding RDA models

198 against river km after Legendre and Legendre (2012).

199

200 Results

201

202 Morphometric data

203

204 The largest mesh sizes were observed in *C. curvispinum* (6.33-18.35 μm; Fig. 2). The inclusion of

205 body length as a fixed variance weight was supported (Table S1), whereas the effects of 'gender',

206 'sampling site', and all interaction terms could be neglected (Table S2). Among-individual variance

207 was high and within-individual variation was also considerable, which resulted in a relatively weak

208 but statistically significant body length-dependency (Table 3).

209 The filter mesh size of *C. robustum* ranged between 4.68 and 13.02 μm, increasing asymptotically

210 with body length (Fig. 2). However, non-linear models did not provide a good fit due to the relatively

211 short saturation interval; therefore, we divided the dataset into two approximately linear parts by

212 maximizing the difference between the slopes of the two segments, which allowed comparability with

213 the other two species. Below 5.5 mm, mesh sizes showed a clear linear increase with body length

214 despite considerable among- and within-individual variation (Table 3), whereas the effects of 'gender',

215 'sampling site' and the interaction terms were not significant(Table S2). The inclusion of variance

216 functions in the model was not supported (Table S1). Above 5.5 mm, the effect of body length on

217 filter mesh size was not significant ($P = 0.152$). 'Gender' and 'sampling site' were not included in the

218 model due to the strongly unbalanced design (only females attained sizes larger than ~ 6 mm, and

219 large specimens were rare at river km 104), and the usage of variance functions was not necessary,

220 either (Table S1). Since fixed effects were not included in the model and among-individual variability

221 was moderate, most of the variation was attributable to within-individual differences (Table 3).

222   The filter mesh size of *C. sowinskyi* was the smallest among the three species, ranging between 2.64

223   and 6.87 μm (Fig. 2). The usage of body length as a fixed weight was supported (Table S1), as

224   variance increased considerably with the size of the animals. Filter mesh size showed a clear linear

225   increase with body length, and the interaction between body length and gender also proved significant

226   (0.28, *SE* = 0.05; *P*<0.001), reflecting the fact that males attained smaller body lengths but had a mesh

227   size range similar to females (the effects of 'sampling site' and the interaction terms could be

228   neglected; Table S2). However, for the sake of comparability with the other species, we included only

229   body length in the model shown in Table 3, indicating considerable among-individual, but relatively

230   low within-individual variation.

231   To allow a meaningful interspecific comparison of filter mesh sizes in spite of the considerable effect

232   of body length, we excluded specimens of *C. robustum* larger than 5.5 mm from the model involving

233   all three species. As the effects of 'gender', 'sampling site' and the interaction terms proved

234   insignificant in the single-species models (the body length-gender interaction was significant but

235   negligible compared to interspecific differences in *C. sowinskyi*) , they were not included in the initial

236   model. The usage of a stratified variance structure was supported (Table S1; parameters. *C.*

237   *curvispinum*: 1.20; *C. robustum*: 1; *C. sowinskyi*: 0.38). Body length showed negligible interactions

238   among the species (*P* = 0.805 for *C. curvispinum*, *P* = 0.842 for *C. sowinskyi*), so interspecific

239   differences in filter mesh size could be interpreted as the differences among the intercepts of the fitted

240   lines (fixed effects), which were estimated 2.86 μm (*SE* = 0.37; *P* < 0.001) between *C. curvispinum*

241   and *C. robustum*, and 3.52 μm (*SE* = 0.40; *P* < 0.001) between *C. robustum* and *C. sowinskyi* (Fig. 2).

242

243   Field data

244

245   Three *Chelicorophium* species were recorded during the survey of which *C. curvispinum* was the most

246   common, occurring at 51 sites (169 samples) between river km 2,415 and 18 (Fig. 1) with a maximum

247   density of 5,280 ind./m^2 (median: 42, interquartile range: 10-208; zeros not included). *C. sowinskyi*

248   was found between river km 2,415 and 18 during the survey (38 sites, 106 samples); however, it was

249   missing between river km 1,630 and 1,199 (Fig. 1). It reached extreme high densities (54,835 and

250 43,904 ind./m^2) in two samples taken below the mouth of the River Jantra (river km 532), whereas in

251 other parts of the river its density did not exceed 5,050 ind./m^2 (median: 37, interquartile range: 10-

252 112 including the two extreme values). *C. robustum* was recorded at 37 sites (89 samples) between

253 river km 2,415 and 26 with a notable gap between river km 1,367 and 1,159 (Fig. 1). The highest

254 density of the species was 5,523 ind./m^2 (median: 16, interquartile range: 3-64).

255 The forward selection procedure with $P = 0.05$ adding limit selected TSS, substrate type, current

256 velocity, and total nitrogen concentration of the environmental variables which altogether explained

257 22.7% ($df = 13$, $F = 4.40$, $P < 0.001$) of the total variation, whereas the nineteen selected AEM

258 eigenfunctions accounted for 43.1% ($df = 19$, $F = 7.01$, $P < 0.001$). The overlap between the two

259 variance portions was considerable (16.0%; not testable), hence 6.7% ($df = 13$, $F = 2.35$, $P < 0.001$)

260 and 27.1% ($df = 19$, $F = 4.91$, $P < 0.001$) could be explained exclusively by environmental and spatial

261 variables, respectively. The two variable sets together accounted for 49.7% ($df = 32$, $F = 5.67$, $P <$

262 0.001) of the total variation. With $P = 0.01$ adding limit, the only selected environmental variable was

263 TSS, explaining 13.3% alone ($df = 1$, $F = 24.14$, $P < 0.001$).

264 The Mantel correlogram (Fig. 3) revealed significant positive spatial autocorrelation in the response

265 variables at fine spatial scales (within sites and in the 0-156 river km distance class), which

266 transitioned into significant negative correlation at intermediate distances (156-779 river km). In the

267 largest distance class (934-1,090 river km) autocorrelation was positive again. The selected

268 environmental variables accounted for most of the autocorrelation; the residuals of the environmental

269 RDA model were significantly correlated only within sites. The inclusion of spatial variables

270 successfully eliminated spatial autocorrelation in all distance classes.

271 The first canonical axis of the RDA ($R^2 = 0.409$, $df = 1$, $F = 152.7$, $P < 0.001$) separated *C.*

272 *curvispinum* from *C. sowinskyi*, placing *C. robustum* in an intermediate position (Fig. 4). On the

273 second axis ($R^2 = 0.181$, $df = 1$, $F = 67.6$, $P < 0.001$), however, *C. robustum* differentiated markedly

274 from the other two species. TSS showed the strongest correlation with the first axis among the

275 environmental variables (biplot scores: RDA1: -0.530, RDA2: 0.359), accounting mainly for the

276 separation of *C. curvispinum* from the other two species. Total nitrogen concentration pointed almost

277 exactly in the same direction as TSS; however, its effect was considerably weaker (RDA1: -0.157,

278 RDA2: 0.099). Current velocity (RDA1: -0.188, RDA2: -0.366) was associated mainly with *C.*

279 *robustum*, whereas the centroids of substrate types concentrated around the origin of the ordination

280 plane, indicating a relatively weak differentiation among the species in this regard.

281 The environmentally explainable variance fraction concentrated between river km 1,300 and 1,159 as

282 a result of a peak in TSS coinciding with the absence of *C. sowinskyi* and *C. robustum* (Fig. 5a). The

283 only spatially explainable part of the variance showed a complex distribution along the river with

284 notable peaks in the Iron Gates section and in the vicinity of the delta (Fig. 5b).

285

286 Discussion

287

288 Our measurements revealed considerable differences in the filter mesh sizes among the invasive

289 *Chelicorophium* species.. The relationship between filter mesh size and particle capture efficiency is

290 not evident; particles smaller than the mesh size might be retained, especially when the material of the

291 filter is sticky (Shimeta and Jumars 1991). Nevertheless, clearance rate dropped steeply for particles

292 smaller than the mesh size in *Corophium volutator* (Pallas, 1766) (Møller and Riisgård 2006) in

293 accordance with the particle size distribution of gut contents (Fenchel et al. 1975), suggesting that the

294 primary filtering mechanism in corophiids is sieving (i.e. the mechanical retention of particles larger

295 than mesh size of the filter; Shimeta and Jumars 1991). On the other hand, hydraulic resistance

296 increases with smaller mesh sizes (Cheer and Koehl 1987), implying that less water can be filtered

297 with the same effort; therefore, filters are not efficient at capturing particles considerably larger than

298 the mesh size. Consequently, there is a particle size range for each species where their capture rate is

299 higher than that of the others. Within this range, the species can tolerate a lower resource density than

300 the others, translating into competitive advantage (Chase and Leibold 2003). Nevertheless, a

301 sufficiently wide size distribution of the food particles might allow the coexistence of the species even

302 locally, and spatial heterogeneity in resource availability also might promote their coexistence at the

303 regional scale (Chase and Leibold 2003).

304 Accordingly,the interspecific differences in the filter mesh sizes among the invasive *Chelicorophium*

305 species revealed in our study indicate niche differentiation by food particle size. Since spatial

306 differences were not detected over several hundred river km distances, our results can be considered as

307 representative for the Lower Danube. Nevertheless, we expect that a similar pattern will be found

308 wherever the three species coexist, and considerable differences will be observed only in situations

309 where some of the species are missing, implying release from competitive pressure on the others.

310 Our study identified sources of variation in filter mesh size within the species, as well. The body

311 length dependency of the character was marked in all three species, most likely reflecting ontogenetic

312 changes. However, since repeated measurements on cohorts were not made in our study, alternative

313 explanations (i.e. differences among cohorts) cannot be excluded with full certainty. Slight

314 differences could be observed between genders, too, especially in *C. sowinskyi*. However,

315 these are not likely to have ecological relevance; they might merely reflect the considerable

316 sexual dimorphism in body proportions (i.e. males attain smaller standard lengths but have

317 larger antennae). The ratio of unexplained variance in the models was also considerable,

318 especially among and within the individuals of *C. curvispinum*, calling for further analyses.

319 Field data indicated the relevance of suspended matter in the niche differentiation among invasive

320 Ponto-Caspian *Chelicorophium* species; the majority of the environmentally explained variance was

321 attributable to this factor. Nevertheless, since only the overall quantity of suspended matter could be

322 included in the analysis, its role is not trivial. As the morphological differences suggest, considerable

323 explanatory power could be expected only from detailed data on the qualitative composition and size

324 distribution of suspended particles. The effect of TSS was attributable mainly to the coincidence of

325 peak values with the absence of *C. robustum* and *C. sowinskyi* in the Serbian river section (Fig. 5a).

326 Since the downstream spread of *C. robustum* was still in progress at the time of the survey, its absence

327 might not necessarily be the result of environmental factors. On the other hand, unfavorable suspended

328 matter composition in this river section (combined with current velocity and sediment composition;

329 Borza et al. 2015) could explain why the upstream distributional limit of the species used to be here

330 for a long time. Recently, the species has been found at some additional sites in this river section (river

331 km 1,334; Žganec et al., unpublished data); however, it is still early to draw conclusions in this

332 question.

The distributional gap of *C. sowinskyi* was not related to any of the environmental factors included in the analysis. However, former data show the eutrophic character of the river section downstream of Budapest (Dokulil and Donabaum 2014), which might provide a historical explanation. The central sewage treatment plant of the city began to operate only in 2010, so the species might not have had the time to respond to the changed conditions at the time of the survey. Its record downstream of the city might be an indication of its incipient spread (Borza et al. 2015).

High suspended matter load, however, does not necessarily lead to *C. curvispinum* dominance; the extreme high density of *C. sowinskyi* downstream of the River Jantra mouth might be related to the high TSS values in this tributary (125 mg/l during the survey). Unfortunately, TSS was measured at only one point per site in the middle of the channel during the survey, so the connection is not reflected in the data. Nevertheless, the peak densities recorded during the survey are still well below the values recorded in the eutrophic River Rhine shortly after the invasion of *C. curvispinum* (up to 750,000 ind./m^2; Van den Brink et al. 1993). The generally low density values of *Chelicorophium* species and their strong response to the extra suspended matter load of tributaries suggest strong food limitation in most parts of the Danube at the present time.

The explanatory power of the remaining variables was rather low; therefore, our field data do not provide firm evidence for their importance in the niche differentiation of invasive *Chelicorophium* species. The weak effect of total nitrogen concentration could not be separated from that of TSS, and current velocity as well as substrate types also might be related to food availability, so they might not necessarily represent independent niche axes. On the contrary, we assume that the larger body size of *C. robustum* might be relevant to the coexistence of the species. In this case, various factors might be potentially involved, including microhabitat use, generation time, predation risk, or interference competition. Nevertheless, these can be expected only to modulate, not to overcome the differentiation by food particle size.

In summary, differences in their filter mesh sizes allow a stable coexistence among the three invasive *Chelicorophium* species, where their abundance is primarily determined by the quantity, quality, and size distribution of suspended matter. Consequently, the joint impact of the three species – as compared to *C. curvispinum* alone – is a more effective resource utilization, resulting in a stronger

361 benthic-pelagic coupling. Inferring from their smaller filter mesh sizes, the impact of the two recent

362 invaders can be expected to be most pronounced if suspended matter is dominated by relatively small

363 (< ~10 μm) food particles. It would be useful to compare invasive and presently non-invasive

364 *Chelicorophium* species, which could provide insight into the factors of invasion success and allow a

365 more accurate assessment of future invasion risks within the genus (Borza et al. 2017b). Similarly, to

366 obtain a more complete overview about the utilization of suspended matter in the ecosystems

367 concerned, it would be important to study all co-occurring filter feeding species jointly.

368

369 References

370

371 Altermatt F, Alther R, Fišer C, Jokela J, Konec M, Küry D, Mächler E, Stucki P, Westram AM (2014)

372   Diversity and distribution of freshwater amphipod species in Switzerland (Crustacea:

373   Amphipoda). PloS One 9:e110328

374 Atkinson CL, Vaughn CC, Forshay KJ, Cooper JT (2013) Aggregated filter-feeding consumers alter

375   nutrient limitation: consequences for ecosystem and community dynamics. Ecology 94:1359–

376   1369

377 Bernauer D, Jansen W (2006) Recent invasions of alien macroinvertebrates and loss of native species

378   in the upper Rhine River, Germany. Aquat Invasions 1:55–71

379 Bernerth H, Dorow S (2010) *Chelicorophium sowinskyi* (Crustacea, Amphipoda) ist aus der Donau in

380   den Main vorgedrungen - Anmerkungen zur Verbreitung und Morphologie der Art.

381   Lauterbornia 70:53–71

382 Bernerth H, Tobias W, Stein S (2005) Faunenwandel im Main zwischen 1997 und 2002 am Beispiel

383   des Makrozoobenthos. In: Faunistisch-ökologische Untersuchungen des Forschungsinstitutes

384   Senckenberg im hessischen Main. Hessisches Landesamt für Umwelt und Geologie,

385   Wiesbaden, pp 15–87

386 Bij de Vaate A, Jażdżewski K, Ketelaars HAM, Gollasch S, Van der Velde G (2002) Geographical

387   patterns in range extension of Ponto-Caspian macroinvertebrate species in Europe. Can J Fish

388   Aquat Sci 59:1159–1174

389 Blanchet FG, Legendre P, Borcard D (2008a) Modelling directional spatial processes in ecological

390   data. Ecol Model 215:325–336

391 Blanchet FG, Legendre P, Borcard D (2008b) Forward selection of explanatory variables. Ecology

392   89:2623–2632

393 Blanchet FG, Legendre P, Maranger R, Monti D, Pepin P (2011) Modelling the effect of directional

394   spatial ecological processes at different scales. Oecologia 166:357–368

395 Borza P (2011) Revision of invasion history, distributional patterns, and new records of Corophiidae

396   (Crustacea: Amphipoda) in Hungary. Acta Zool Acad Sci Hung 57:75–84

397 Borza P, Csányi B, Huber T, Leitner P, Paunović M, Remund N, Szekeres J, Graf W (2015)

398   Longitudinal distributional patterns of Peracarida (Crustacea, Malacostraca) in the River

399   Danube. Fundam Appl Limnol 187:113–126

400 Borza P, Csányi B, Paunović M (2010) Corophiids (Amphipoda, Corophioidea) of the River Danube

401   The Results of a Longitudinal Survey. Crustaceana 83:839–849

402 Borza P, Huber T, Leitner P, Remund N, Graf W (2017a) Current velocity shapes co-existence

403   patterns among invasive *Dikerogammarus* species. Freshw Biol 62:317–328

404 Borza P, Huber T, Leitner P, Remund N, Graf W (2017b) Success factors and future prospects of

405   Ponto–Caspian peracarid (Crustacea: Malacostraca) invasions: Is "the worst over"? Biol

406   Invasions 19:1517–1532

407 Brönmark C, Malmqvist B (1982) Resource partitioning between unionid mussels in a Swedish lake

408   outlet. Ecography 5:389–395

409   Chase JM, Leibold MA (2003) Ecological niches: linking classical and contemporary approaches.

410   University of Chicago Press, Chicago and London

411   Cheer AYL, Koehl MAR (1987) Paddles and rakes: fluid flow through bristled appendages of small

412   organisms. J Theor Biol 129:17–39

413   Dokulil MT, Donabaum U (2014) Phytoplankton of the Danube river: Composition and long-term

414   dynamics. Acta Zool Bulg Suppl 7:147–152

415   Fenchel T, Kofoed LH, Lappalainen A (1975) Particle size-selection of two deposit feeders: the

416   amphipod *Corophium volutator* and the prosobranch *Hydrobia ulvae*. Mar Biol 30:119–128

417   Forcellini M (2012) First record of the Ponto-Caspian invasive crustacean *Chelicorophium sowinskyi*

418   (Martinov, 1924) (Amphipoda, Corophiidae) in the French Rhône River. Crustaceana

419   85:1781–1785

420   Griffiths JR, Kadin M, Nascimento FJA, Tamelander T, Törnroos A, Bonaglia S, Bonsdorff E,

421   Brüchert V, Gårdmark A, Järnström M, Kotta J, Lindegren M, Nordström MC, Norkko A,

422   Olsson J, Weigel B, Žydelis R, Blenckner T, Niiranen S, Winder M (2017) The importance of

423   benthic-pelagic coupling for marine ecosystem functioning in a changing world. Glob Change

424   Biol 23: 2179–2196

425   Hellmann C, Worischka S, Mehler E, Becker J, Gergs R, Winkelmann C (2015) The trophic function

426   of *Dikerogammarus villosus* (Sowinsky, 1894) in invaded rivers: a case study in the Elbe and

427   Rhine. Aquat Invasions 10:385–397

428   Hering D, Moog O, Sandin L, Verdonschot PF (2004) Overview and application of the AQEM

429   assessment system. Hydrobiologia 516:1–20

430   Higgins SN, Vander Zanden MJ (2010) What a difference a species makes: a meta–analysis of

431   dreissenid mussel impacts on freshwater ecosystems. Ecol Monogr 80:179–196

432   Jones LA, Ricciardi A (2005) Influence of physicochemical factors on the distribution and biomass of

433   invasive mussels (*Dreissena polymorpha* and *Dreissena bugensis*) in the St. Lawrence River.

434   Can J Fish Aquat Sci 62:1953–1962

435   Kang C-K, Choy EJ, Hur Y-B, Myeong J-I (2009) Isotopic evidence of particle size-dependent food

436   partitioning in cocultured sea squirt *Halocynthia roretzi* and Pacific oyster *Crassostrea gigas*.

437   Aquat Biol 6:289–302

438   Kelleher B, Bergers PJM, Van den Brink FWB, Giller PS, Van der Velde G, Bij de Vaate A (1998)

439   Effects of exotic amphipod invasions on fish diet in the Lower Rhine. Arch Für Hydrobiol

440   143:363–382

441   Labat F, Piscart C, Fontan B (2011) First records, pathways and distributions of four new Ponto-

442   Caspian amphipods in France. Limnologica 41:290–295

443   Lefcheck JS (2016) piecewiseSEM: Piecewise structural equation modelling in r for ecology,

444   evolution, and systematics. Methods Ecol Evol 573–579

445   Legendre P, Gallagher ED (2001) Ecologically meaningful transformations for ordination of species

446   data. Oecologia 129:271–280

447   Legendre P, Legendre LF (2012) Numerical ecology. 3rd English edition. Elsevier, Amsterdam

448   Lesser MP, Shumway SE, Cucci T, Smith J (1992) Impact of fouling organisms on mussel rope

449   culture: interspecific competition for food among suspension-feeding invertebrates. J Exp Mar

450   Biol Ecol 165:91–102

451   Møller LF, Riisgård HU (2006) Filter feeding in the burrowing amphipod *Corophium volutator*. Mar

452   Ecol Prog Ser 322:213–224

453   Nakagawa S, Schielzeth H (2013) A general and simple method for obtaining R^2 from generalized

454   linear mixed-effects models. Methods Ecol Evol 4:133–142

455 Noordhuis R, van Schie J, Jaarsma N (2009) Colonization patterns and impacts of the invasive

456   amphipods *Chelicorophium curvispinum* and *Dikerogammarus villosus* in the IJsselmeer area,

457   The Netherlands. Biol Invasions 11:2067–2084

458 Oksanen J, Blanchet FG, Kindt R, Legendre P, Minchin PR, O'Hara RB, Simpson GL, Solymos P,

459   Stevens MHH, Wagner H (2017) vegan: Community Ecology Package. R package version

460   2.4-3. http://CRAN.R-project.org/package=vegan

461 Pinheiro J, Bates D, DebRoy S, Sarkar D, R Core Team (2016) nlme: Linear and Nonlinear Mixed

462   Effects Models. R package version 3.1-125, http://CRAN.R-project.org/package=nlme.

463 R Core Team (2016) R: A language and environment for statistical computing. R Foundation for

464   Statistical Computing, Vienna, Austria. URL http://www.R-project.org/

465 Riisgård HU, Larsen PS (2010) Particle capture mechanisms in suspension-feeding invertebrates. Mar

466   Ecol Prog Ser 418:255–293

467 Rohlf FJ (2015) tpsDig, Digitize Landmarks and Outlines, version 2.22. Department of Ecology and

468   Evolution, State University of New York, Stony Brook.

469 Shimeta J, Jumars PA (1991) Physical mechanisms and rates of particle capture by suspension-

470   feeders. Oceanogr Mar Biol - Annu Rev 29:l–257

471 Sousa R, Novais A, Costa R, Strayer DL (2014) Invasive bivalves in fresh waters: impacts from

472   individuals to ecosystems and possible control strategies. Hydrobiologia 735:233–251

473 Svensson JR, Marshall DJ (2015) Limiting resources in sessile systems: food enhances diversity and

474   growth of suspension feeders despite available space. Ecology 96:819–827

475 Van den Brink FWB, Van der Velde G, Bij de Vaate A (1993) Ecological aspects, explosive range

476   extension and impact of a mass invader, *Corophium curvispinum* Sars, 1895 (Crustacea:

477   Amphipoda), in the Lower Rhine (The Netherlands). Oecologia 93:224–232

478   Van der Velde G, Paffen BGP, Van den Brink FWB, Bij de Vaate A, Jenner HA (1994) Decline of

479   zebra mussel populations in the Rhine. Naturwissenschaften 81:32–34

480   Van Riel MC, Van der Velde G, Rajagopal S, Marguillier S, Dehairs F, Bij de Vaate A (2006) Trophic

481   relationships in the Rhine food web during invasion and after establishment of the Ponto-

482   Caspian invader *Dikerogammarus villosus*. Hydrobiologia 565:39–58

483   Wallace JB, Webster JR, Woodall WR (1977) The role of filter feeders in flowing waters. Arch Für

484   Hydrobiol 79:506–532

485   Zhang X, Liu Z, Jeppesen E, Taylor WD, Rudstam LG (2016) Effects of benthic-feeding common

486   carp and filter-feeding silver carp on benthic-pelagic coupling: implications for shallow lake

487   management. Ecol Eng 88:256–264

488   Zuur AF, Ieno EN, Walker NJ, Saveliev AA, Smith GM (2009) Mixed effects models and extensions

489   in ecology with R, Springer Science and Business Media. New York

490

491 **Tables**

492

493 **Table 1** Number of specimens involved in the morphometric measurements. *C. robustum* was divided

494 into two size classes due to the non-linear body length dependence of its filter mesh size (see text)

Species	river km 532	river km 375	river km 104	Σ
C. curvispinum		23 (9 ♂, 13 ♀, 1 juv.)	13 (7 ♂, 6 ♀)	36
C. robustum (< 5.5 mm)		15 (6 ♂, 7 ♀, 2 juv.)	8 (3 ♂, 5 ♀)	23
C. robustum (≥ 5.5 mm)		11 (3 ♂, 8 ♀)	2 (2 ♀)	13
C. sowinskyi	20 (9 ♂, 10 ♀, 1 juv.)		10 (5 ♂, 5 ♀)	30

495

496 **Table 2** Definitions of substrate types used in the study

497

Substrate type	Definition
riprap	rocks of variable size, artificial
macrolithal	blocks, large cobbles; grain size 20 cm to 40 cm
mesolithal	cobbles; grain size 6 cm to 20 cm
microlithal	coarse gravel; grain size 2 cm to 6 cm
akal	fine to medium-sized gravel; grain size 0.2 cm to 2 cm
psammal	sand; grain size 0.063-2 mm
psammopelal	sand and mud
pelal	mud (organic); grain size < 0.063 mm
argyllal	silt, loam, clay (inorganic); grain size < 0.063 mm
macrophytes	submerged macrophytes, including moss and Characeae
xylal	tree trunks, dead wood, branches, roots

498

499 **Table 3** Parameters and variance components of the single-species linear mixed-effects models

500

Species	Intercept (μm)	Slope (body length)	Body length-dependency (= fixed effects)	Among-individual variation (= random effects)	Within-individual variation (= residual)
C. curvispinum	7.51 (*SE* = 1.42; *P* < 0.001)	1.02 (*SE* = 0.40; *P* = 0.015)	0.15	0.80	0.05
C. robustum (< 5.5 mm)	5.02 (*SE* = 0.64; *P* < 0.001)	0.92 (*SE* = 0.16; *P* < 0.001)	0.41	0.27	0.32
C. robustum (≥ 5.5 mm)	9.90 *(SE* = 0.08; *P* < 0.001)	not significant	-	0.11	0.89
C. sowinskyi	1.77 (*SE* = 0.45; *P* < 0.001)	0.83 (*SE* = 0.14; *P* < 0.001)	0.52	0.44	0.04

501 **Figure captions**

502

503 **Fig. 1** Occurrences of *Chelicorophium* species in the River Danube during Joint Danube Survey 3

504 (multi-habitat samples only). White squares: *C. curvispinum*, grey circles: *C. sowinskyi*, black

505 triangles: *C. robustum*. The dark shaded area corresponds to the River Danube basin. Codes of the

506 riparian countries: DE: Germany, AT: Austria, SK: Slovakia, HU: Hungary, HR: Croatia, RS: Serbia,

507 RO: Romania, BG: Bulgaria, MD: Moldova, UA: Ukraine

508

509 **Fig. 2** Filter mesh sizes of *Chelicorophium* species as a function of body length. Lines represent the

510 fitted values of the single-species linear mixed-effects models

511

512 **Fig. 3** Mantel correlograms of the response variables, the residuals of the environmental model (E),

513 and the residuals of the environmental and spatial model (E + S). The distance class at 0 river km

514 corresponds to within-site distances. Solid symbols indicate significant correlations (*: $P < 0.05$, **: P

515 < 0.01, ***: $P < 0.001$). Numbers on the top of the graph indicate the number of pairs involved in the

516 calculation of correlations for each distance class. Symbols are connected only to visualize the trends

517

518 **Fig. 4** Triplot showing the results of the RDA including both environmental and spatial explanatory

519 variables ('*WA*' scores, species scaling). Cc: *C. curvispinum*, Cs: *C. sowinskyi*, Cr: *C. robustum*.

520 Substrate types: AKA: akal, ARG: argyllal, MAL: macrolithal, MEL: mesolithal, MIL: microlithal,

521 MPH: macrophytes, PEL: pelal, PPE: psammopelal, PSA: psammal, RIP: rip-rap, XYL: xylal. Arrows

522 represent continuous environmental variables (cur: current velocity, tss: total suspended solids, toN:

523 total nitrogen). AEM eigenfunctions are not shown for the sake of perspicuity

524

525 **Fig. 5** The distribution of the environmentally (a) and the only spatially (b) explainable part of

526 variance (i.e. the fitted site scores of the first canonical axis in the corresponding RDA models) along

527 the investigated river section. Solid lines represent smoothed splines (function 'smooth.spline' in R)

528   with a smoothing parameter of 0.5. Total suspended solid (TSS) values are shown in (a) for
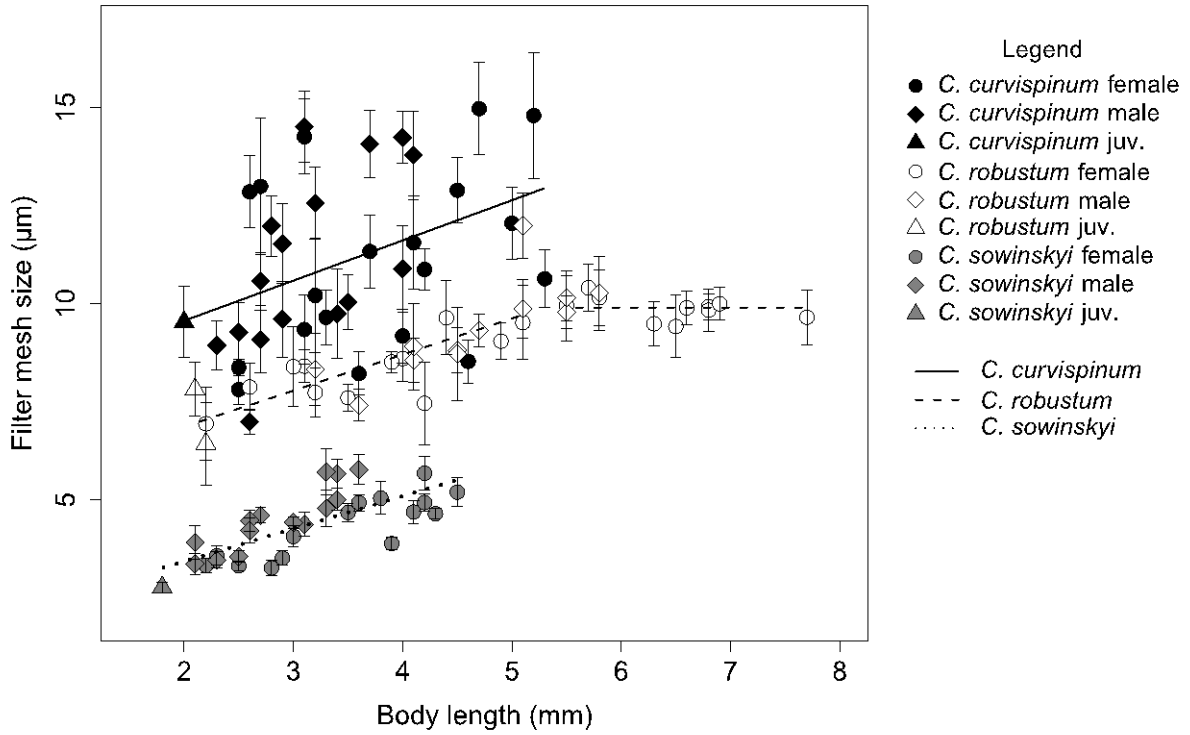
529   comparison
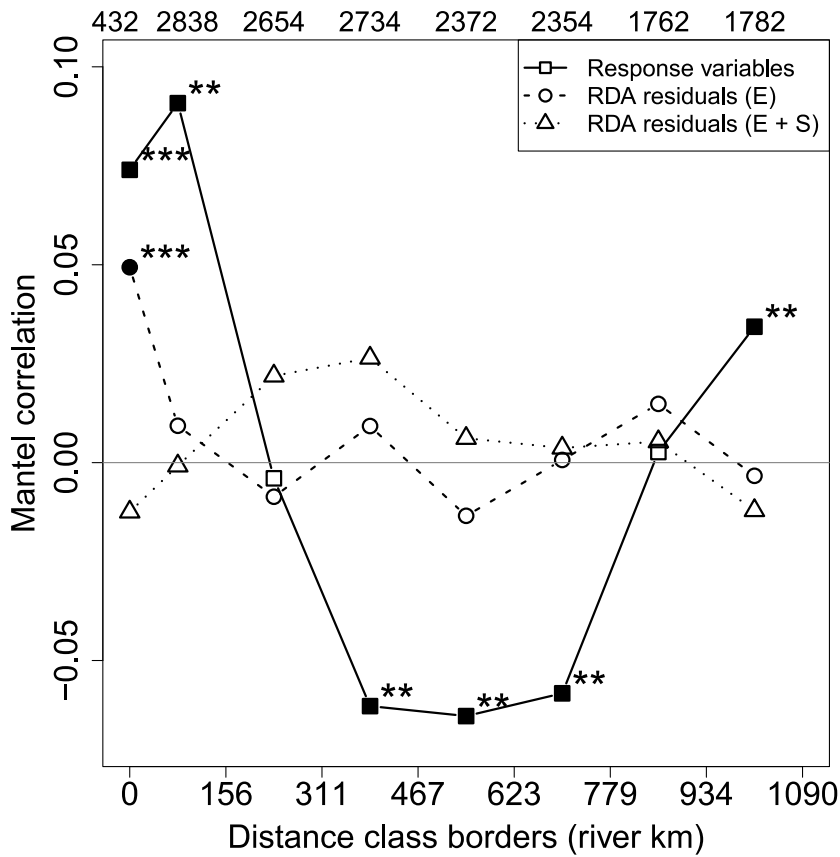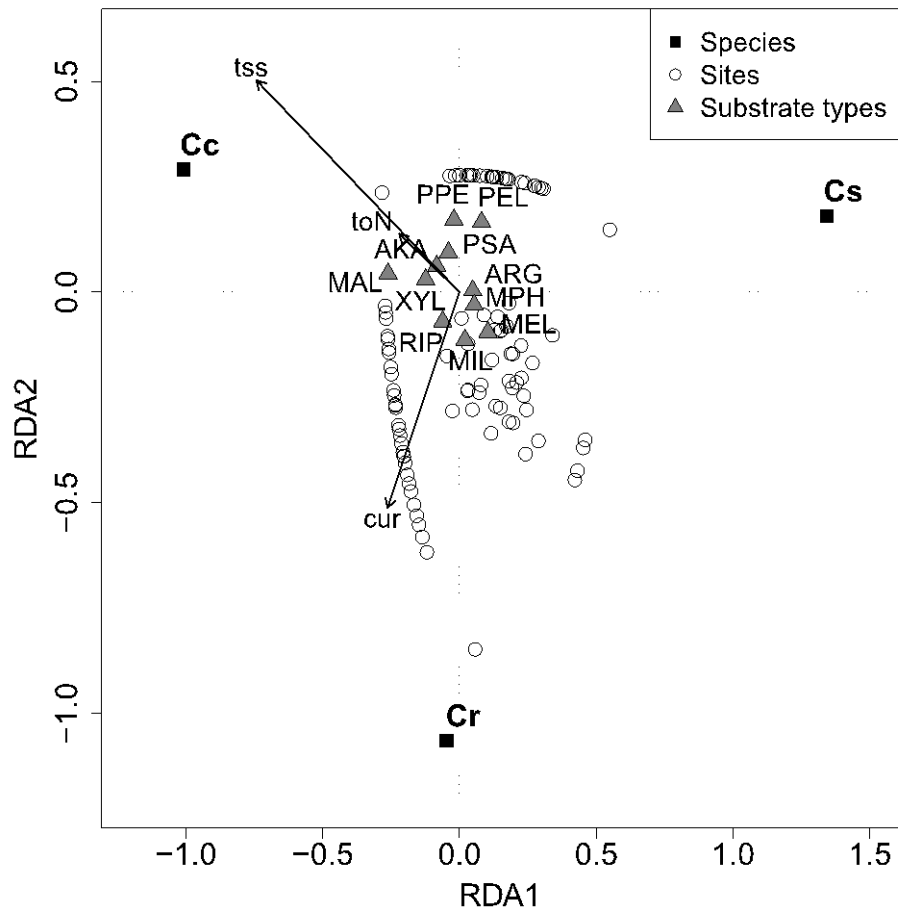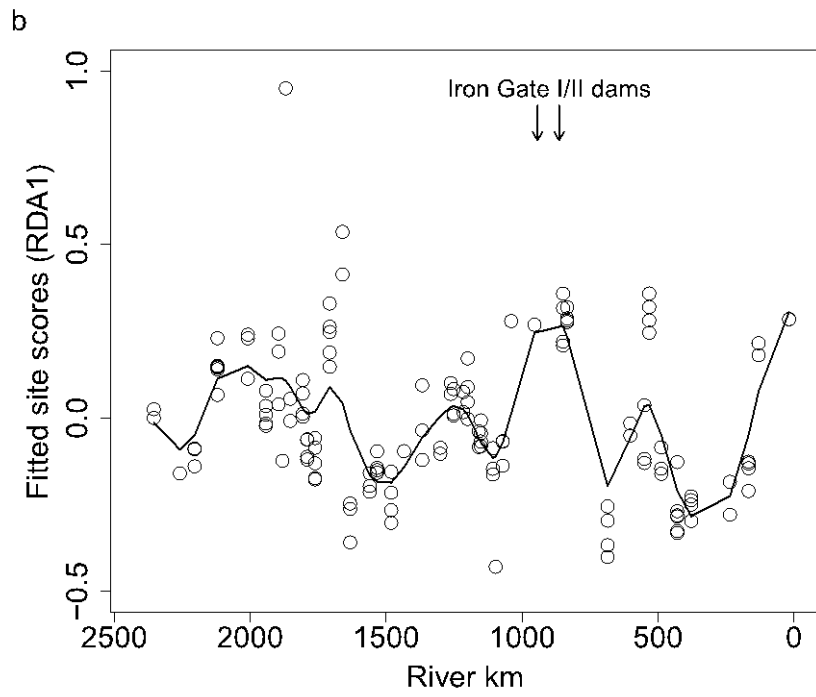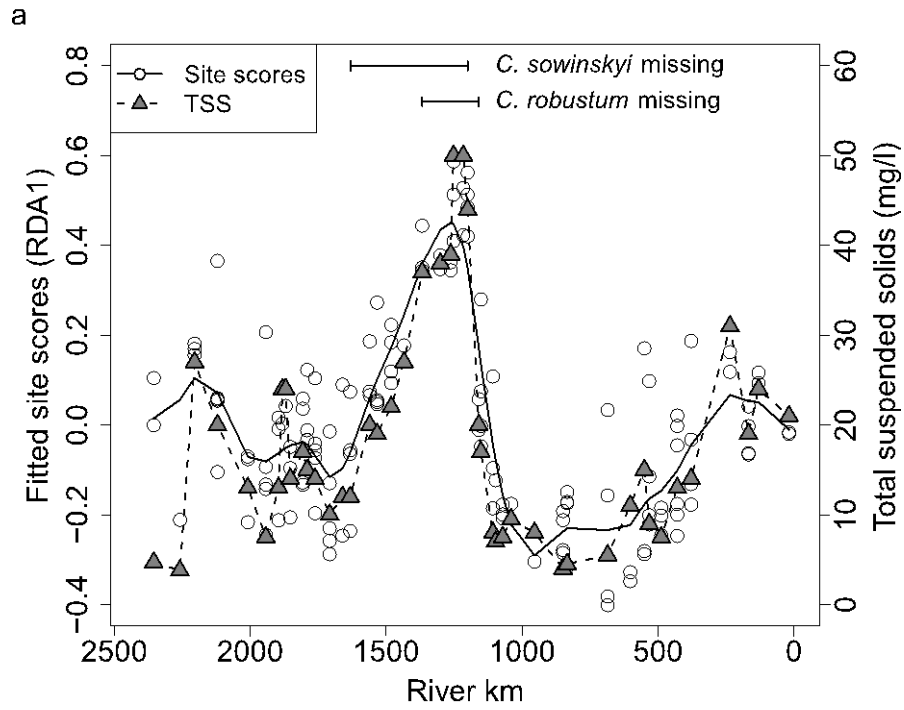
530   Figures

531   Fig. 1
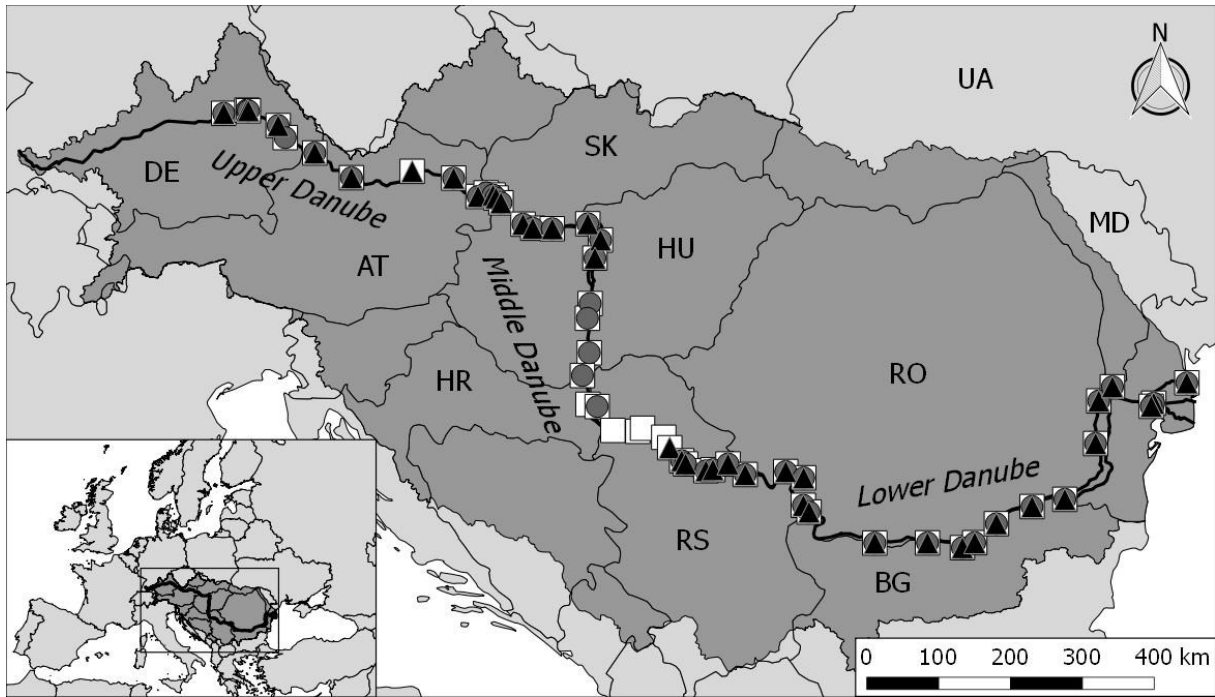
532

533   Fig. 2

534

535   Fig. 3

536

537   Fig. 4

538

539   Fig. 5

a

b

540